Paleoenvironmental history of the West Baray, Angkor (Cambodia)

Mary Beth Day[a,1], David A. Hodell[b], Mark Brenner[c], Hazel J. Chapman[a], Jason H. Curtis[d], William F. Kenney[c], Alan L. Kolata[e], and Larry C. Peterson[f]

[a]Department of Earth Sciences, Downing Street, University of Cambridge, Cambridge, UK, CB2 3EQ; [b]Department of Earth Sciences and Godwin Laboratory for Palaeoclimate Research, Downing Street, University of Cambridge, Cambridge, UK, CB2 3EQ; [c]Department of Geological Sciences and Land Use and Environmental Change Institute, P.O. Box 112120, University of Florida, Gainesville, FL, 32611; [d]Department of Geological Sciences, P.O. Box 112120, University of Florida, Gainesville, FL, 32611; [e]Department of Anthropology, 1126 East 59th Street, University of Chicago, Chicago, IL, 60637; and [f]Rosenstiel School of Marine and Atmospheric Science, 4600 Rickenbacker Causeway, University of Miami, Miami, FL, 33149

Edited by Mark H Thiemens, University of California San Diego, La Jolla, CA, and approved November 22, 2011 (received for review July 15, 2011)

Angkor (Cambodia) was the seat of the Khmer Empire from the 9th to 15th century AD. The site is noted for its monumental architecture and complex hydro-engineering systems, comprised of canals, moats, embankments, and large reservoirs, known as barays. We infer a 1,000-y, ^{14}C-dated paleoenvironmental record from study of an approximately 2-m sediment core taken in the largest Khmer reservoir, the West Baray. The baray was utilized and managed from the time of construction in the early 11th century, through the 13th century. During that time, the West Baray received relatively high rates of detrital input. In the 14th century, linear sedimentation rates diminished by an order of magnitude, yielding a condensed section that correlates temporally with episodes of regional monsoon failure during the late 14th and early 15th century, recorded in tree ring records from Vietnam. Our results demonstrate that changes in the water management system were associated with the decline of the Angkorian kingdom during that period. By the 17th century, the West Baray again functioned as a limnetic system. Ecologic and sedimentologic changes over the last millennium, detected in the baray deposits, are attributed to shifts in regional-scale Khmer water management, evolving land use practices in the catchment, and regional climate change.

isotope geochemistry | paleolimnology | collapse

Angkor was established as the capital of the Khmer Empire in the ninth century and became the most extensive preindustrial urban complex in the world (Fig. 1) (1, 2). Although best known for its monumental architecture, particularly the Angkor Wat temple, one of Angkor's most impressive features is its elaborate water management system. A network of reservoirs, channels, moats, and embankments extended over approximately 1,000 km^2. The city's location in lowland Southeast Asia (Cambodia) meant the Khmer had to contend with seasonal monsoon rainfall. The complex water management network enabled the Khmer to collect, store, and release water as needed (2–5). Barays, in particular, were used to store excess water delivered during the summer monsoon. This water could later be distributed to paddy fields between the main temple area around Angkor Wat and Tonle Sap Lake, in the event of a water shortage caused by insufficient rainfall (2). Some scholars have argued that the water management system was purely symbolic (6, 7), but it was probably used for a combination of flood control, irrigation, and ritual purposes (1, 2, 8–10). The water management network was likely a multipurpose architectonic feature serving different functions at different times (3).

The decline of the Khmer Empire in the 14th to 15th centuries has been attributed to several factors, including war, conversion to Theravada Buddhism, changing regional trade patterns, overpopulation, and environmental stress (11). Recent evidence suggests that the water management system may have been insufficient to cope with changing hydrological conditions (1, 3, 5, 12). Alterations, breaches, and failures within the network have been documented and hint at deterioration of the hydraulic infrastructure (1, 2, 12, 13). Tree ring records from Vietnam indicate extended periods of severe drought punctuated by unusually rainy intervals during the late 14th and early 15th centuries (12) (Fig. 2*B*). Such intense variability in multidecadal precipitation may have overwhelmed the capabilities of the water management network. Intense droughts occurred during the transition from the relatively wet Medieval Climate Anomaly (MCA) to the drier Little Ice Age (LIA) and were associated with a southward shift of the Intertropical Convergence Zone (ITCZ) as well as intensified El-Niño-like warming of the tropical Pacific Ocean (12, 14). Monsoon intensity in Southeast Asia, including megadroughts, has been linked to tropical Pacific sea surface temperatures (SSTs) throughout the last millennium (15). Failure of the hydraulic network during a period of extreme rainfall variation may have been a factor in the decline of Angkor.

The West Baray (8 × 2 km) is the largest of the four baray constructed at Angkor, and the only one that holds water today (Fig. 1). The baray floor inclines gently from the northeast to the southwest with an elevation difference of approximately 8 m between the northeast and southwest corners (16) (Fig. S1). If filled to its current maximum capacity, the baray would hold 53 million m^3 of water (16). It is generally assumed the baray was built in the first half of the 11th century, though the precise date is unknown (11). The barays were constructed by building embankments around the intended perimeter using earth acquired by digging trenches inside the perimeter of the baray (5). The primary (65%) source of water and sediment to the West Baray is the Siem Reap River; the remaining 35% of the hydrologic input derives from direct precipitation (16, 17). The Siem Reap River, one of three river catchments in the greater Angkor area today, drains an area that includes the Kulen Hills. This, however, was not always the case. In pre-Angkorian times, only the Puok River and Roluos River catchments existed (5). The Puok River originally emerged from the Kulen Hills but was cut off when the third catchment was formed with the construction of the Siem Reap Channel in the 10th century (prior to the creation of the West Baray) (5, 13). The West Baray received water from rainfall and feeder channels that diverted water from the rivers into central Angkor (2–5). A series of canals channelled water to the northeast corner of the baray, where a 25-m wide channel carried water and sediment into the reservoir (4). A grid of channels off the southwest corner of the West Baray, along with two other channels, directed water toward Tonle Sap Lake. One canal

Author contributions: M.B.D., D.A.H., M.B., J.H.C., and A.L.K. designed research; M.B.D., D.A.H., M.B., H.J.C., J.H.C., W.F.K., and A.L.K. performed research; H.J.C., W.F.K., and L.C.P. contributed new reagents/analytic tools; M.B.D., D.A.H., M.B., H.J.C., and W.F.K. analyzed data; M.B.D., D.A.H., and M.B. wrote the paper.

The authors declare no conflict of interest.

This article is a PNAS Direct Submission.

[1]To whom correspondence should be addressed. E-mail: mbd33@cam.ac.uk.

This article contains supporting information online at www.pnas.org/lookup/suppl/doi:10.1073/pnas.1111282109/-/DCSupplemental.

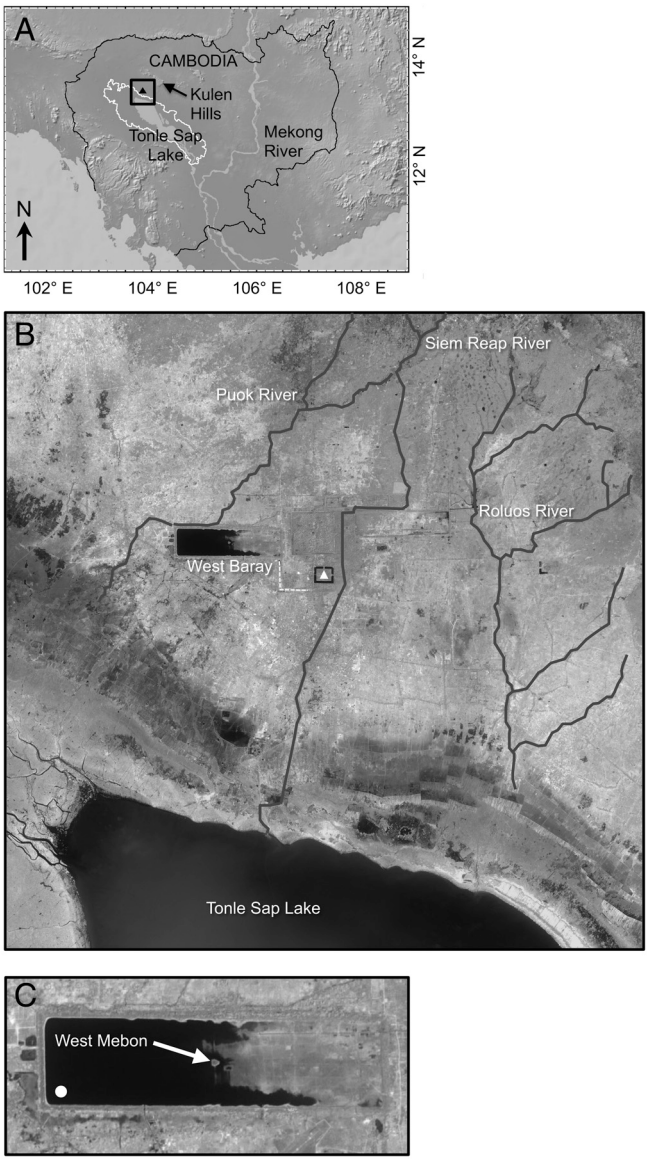

Fig. 1. (*A*) Map of Cambodia. Location of Angkor is indicated by a triangle. The box outlines the location of the satellite image. (*B*) False-color satellite image of the greater Angkor area and the north shore of Tonle Sap Lake. Angkor Wat is indicated by the triangle. The dashed line marks the location of feature CP 807. (*C*) Close up of the West Baray. The circle indicates the location of cores WB1-20-XII-03 MWI-1 and MWI-2, and the location of the West Mebon is indicated. Satellite image obtained by ASTER on 17 February 2004 and accessed from NASA Visible Earth.

flowed southwest on a direct route to the lake and the other flowed southeast. The various channels were likely used to disperse water from the reservoir to the paddy fields south of the West Baray and the main temple area. Sediments that accumulated in the West Baray since its construction record variations in natural hydrologic conditions and Khmer water management practices.

Here we report elemental and isotopic data from an approximately 2-m core taken in the deep, southwest corner of the baray (Fig. 1*C*) and infer local paleoenvironmental changes in response to both natural and anthropogenic forcing. Changes in sediment geochemistry and the rate of sediment accumulation were used to infer the sources and amounts of sediment delivered to the baray, which changed in response to climate variations and Khmer water management strategies. C and N isotopes and elemental ratios (C, N, P) were used to reconstruct changes in the ecology of the baray. Our sedimentologic and geochemical approach elucidates how changes in water and sediment input to the West Baray varied through time and illustrates how the ecology of the system responded to these shifts.

Results

Seven radiocarbon dates constrain the chronology of core WB1-20-XII-03 MWI-1 (Table 1, Fig. 2*A*). A pair of wood and bulk sediment samples was used to evaluate the reliability of bulk sediment dates, as terrestrial plant macrofossils were scarce in the core. Bulk sediment and wood dates from 0.91 to 0.93 m below lake floor (mblf) differed by only 90 ^{14}C y (Table 1) suggesting that bulk sediment in the core yields reliable radiocarbon ages (the *SI Text* provides additional discussion of radiocarbon chronology). The linear sedimentation rate was 1.2 mm/y for the first three centuries after initial baray construction. In the 13th century, linear sedimentation and mass accumulation rates increased sharply, to 6.2 mm/y and 0.88 g/cm^2 y, respectively (Fig. 2*A*, Table 2). The sediment record from about AD 1310 to 1590 is condensed and represents a time period when average sedimentation rate was very low (0.4 mm/y). This approximately 280-y period includes the end of the Angkorian period and a time of enhanced climate variability previously documented by tree ring records (12).

Sediment density peaks near the bottom of the core (approximately 1.9 g/cm^3 below 1.87 mblf, or prior to the mid-10th century) (Fig. S2), indicating the core penetrated to the basal surface of the baray and that the profile contains the entire deposition sequence in this region of the baray. The radiocarbon date of 487 AD below the density peak near the bottom of the core (Fig. S2) confirms this material was deposited centuries before baray construction, and thus the lowermost approximately 4 cm are not considered in our discussion. Sediments become less dense during the 14th and 15th century drought period (approximately 1.0 to 0.8 mblf) and then again from the 18th century (approximately 0.65 mblf) (Fig. 2*C*). Sediment color and density

Table 1. Radiocarbon dates from core WB1-20-XII-03

Accession number	Depth (mblf)	Material	^{14}C y BP	±	Calibrated age(2 sigma)	Probability distribution
SUERC-29786	0.23–0.24	bulk sediment	modern			
CAMS-121348	0.91–0.93	wood	280	35	1491–1602	0.592
					1613–1667	0.374
					1783–1796	0.034
CAMS-144283	0.92–0.93	bulk sediment	370	30	1447–1527	0.576
					1553–1633	0.424
SUERC-29787	1.03–1.04	bulk sediment	700	37	1253–1320	0.743
					1350–1391	0.257
SUERC-29790	1.55–1.56	bulk sediment	804	35	1173–1275	1.000
CAMS-149367	1.86–1.87	bulk sediment	1080	30	894–928	0.278
					934–1017	0.722
SUERC-29791	1.91–1.92	bulk sediment	1576	37	410–564	1.000

Ages were calibrated using Calib, html version 6.0 (24). BP, before present.

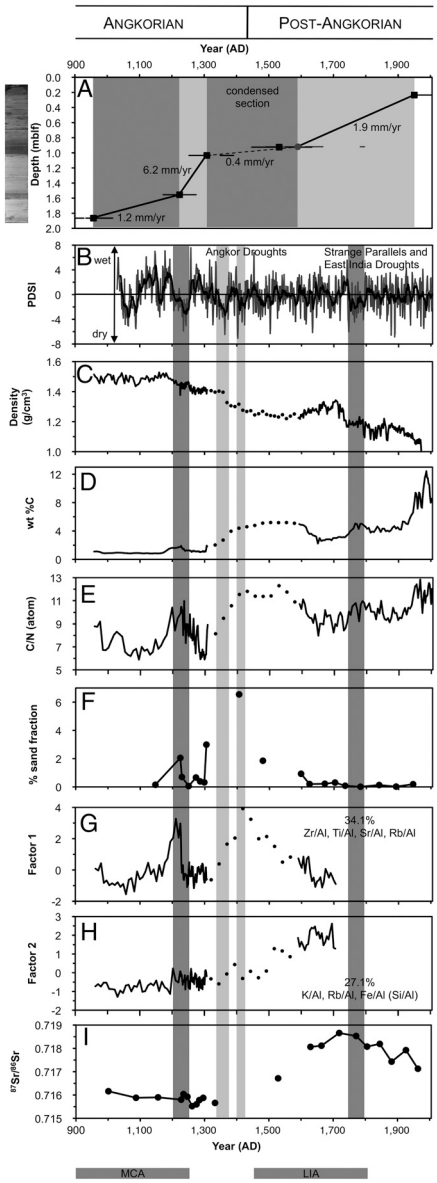

Fig. 2. Summary diagram comparing geochemical and physical variables in Core WB1-20-XII-03 MWI-1 with Palmer Drought Severity Index (PDSI) reconstruction from the Vietnam tree ring record (*B*) (12). Interval mean linear sedimentation rates (mm yr^{-1}) (based on calibrated ^{14}C ages) are noted on the age-depth plot (*A*). Squares represent weighted mean of calibrated bulk sediment dates and the circle signifies the weighted mean of a calibrated wood date. Error bars indicate full range of possible calendar year solutions for each radiocarbon date. The shaded boxes highlight the different time periods for which linear sedimentation and mass accumulation rates were calculated. Light gray shading in panels *B*–*I* indicate the Angkor Droughts (1345–1365, 1401–1425) as defined by Buckley et al. (12), and darker gray shading indicates other drought episodes, including the 13th century drought (12) and the Strange Parallels (1756–1768) and East India (1792–1796) droughts, as defined by Cook et al. (15). Data points acquired within the condensed section of the core (indicated in top panel) are shown as individual points. wt% C and C/N for the last approximately 300 y of the record were measured on core WB1-20-XII-03 MWI-2 (*D*, *E*). For scanning XRF factor analysis, element ratios represented are listed from strongest to weakest loading, with parentheses denoting a negative loading. The percent total variance explained by each factor is indicated (*G*, *H*). The approximate ranges of the MCA and LIA are marked by gray bars.

vary according to organic C content (Fig. S2). Carbonate was undetectable in the West Baray sediments, thus weight %C represents organic C (Fig. 2*D*). Sediment color and organic C content

Table 2. Linear sedimentation rates and mass accumulation rates for core WB1-20-XII-03 MWI-1

Depth (mblf)	Years (AD)	Linear sedimentation rate (mm/y)	Mass accumulation rate (g/cm^2 y)
0.235–0.92	1590–1950	1.9	0.23
0.92–1.035	1308–1590	0.4	0.05
1.035–1.555	1224–1308	6.2	0.88
1.555–1.865	958–1224	1.2	0.19

change abruptly in the early 14th century (approximately 1.03 mblf). In general, sediments deposited during the 10th to 14th centuries (below approximately 1.03 mblf) are light in color and low in organic C, whereas sediments dating from the 15th to 20th centuries (above approximately 1.03 mblf) are darker and higher in organic C content. Superimposed on this general trend are three horizons of darker, higher organic content sediments that were deposited during the early to middle 13th century (approximately 1.60 to 1.50 mblf), between approximately 1320 and 1625 AD (approximately 1.03 to 0.85 mblf), and the mid- to late 18th century (approximately 0.6 to 0.5 mblf) (Fig. 2*D*). Each of these horizons corresponds to drought episodes recorded in the Vietnam tree ring record and other regional paleohydrology records (12, 15) (Fig. 2*B*). C/N atom ratios, which are generally higher from the 17th century on, peak during all three drought periods (Fig. 2*E*). The weight % sand fraction (>63 μm by weight) is less than 1% for most of the profile, indicating the fine sediment grain size. During the period of the Angkor droughts, in the 14th and 15th centuries, weight % sand fraction increases to a maximum value of 6.5% in the early 15th century when Angkor collapsed (Fig. 2*F*). The first factor extracted from factor analysis of Al-normalized scanning X-ray fluorescence (XRF) elemental data indicates a geochemical response during the first two drought episodes, marked by elevated Zr/Al, Ti/Al, Sr/Al, and Rb/Al (Fig. 2*G*).

Factor 2 indicates that K/Al, Rb/Al, and Fe/Al values all increase in the upper portion of the core (1500 AD to the end of the scanning XRF record, approximately 1700 AD), whereas Si/Al values decrease (Fig. 2*H*). Sr isotope ratios ($^{87}Sr/^{86}Sr$) show a similar pattern, becoming more radiogenic, i.e., greater, after 1500 AD (Fig. 2*I*, Table S1). Prior to the mid-14th century, $^{87}Sr/^{86}Sr$ values range from 0.71552 to 0.71616, whereas values from the 16th century onward increase from 0.71672 to 0.71866. Sr isotopes were also measured in surface and river sediments collected from the Puok, Siem Reap, and Roluos River basins. The Puok and Roluos Rivers have significantly less radiogenic $^{87}Sr/^{86}Sr$ values than those of the Siem Reap River or the West Baray (Fig. S3). Carbon and nitrogen stable isotope values become more negative from the 14th century on (Fig. 3 *A* and *B*), whereas total phosphorus (TP) concentrations increase from a mean value of 0.23 mg P/g in the 11th to 13th centuries to 0.40 mg P/g since the 16th century (Fig. 3*C*).

Discussion

Sedimentation in the West Baray. We, and others (17–19) have observed that total sediment accumulation in the West and East Barays is generally low (<0.5 m). For example, Penny et al (17) estimate approximately 43 cm of sediment accumulated in the central part of the East Baray (18), whereas Pottier (19) notes that West Baray sediments are no more than 30 cm thick at Koh Ta Meas (1.3 km west of the West Mebon). It would thus appear that, in comparison, the nearly 2-m long core recovered in the southwest part of the West Baray is quite thick. Typical sediment accumulation patterns in reservoirs, however, are consistent with the observed pattern of sediment deposition in the West Baray, and our core was recovered from the region of the baray in which the thickest sediment deposits are expected (see *SI Text* for discussion of reservoir sedimentation patterns).

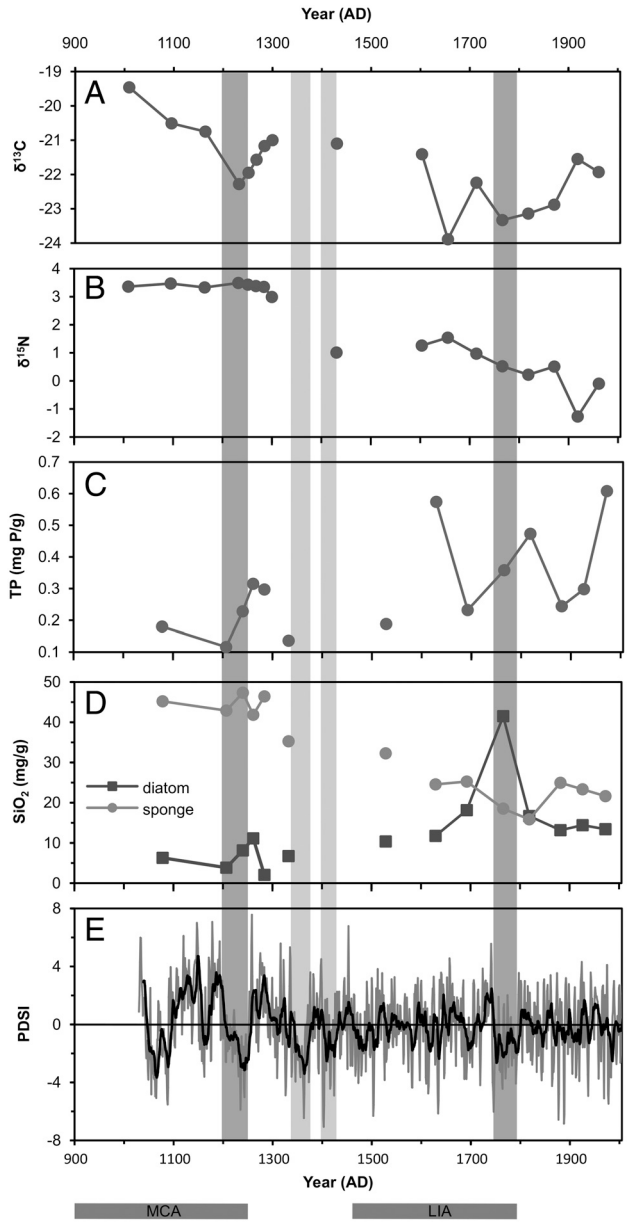

Fig. 3. Carbon (*A*) and nitrogen (*B*) stable isotopes, total P (*C*), and biogenic silica (*D*) from core WB1-20-XII-03 MWI-1, and Palmer Drought Severity Index (PDSI) record (*E*) from Buckley et al. (12). Drought periods are indicated by shading. LIA and MCA are indicated by gray bars.

There is evidence for rapid infill of channels at several locations throughout Angkor, indicating widespread siltation of the water management system during the 13th and 14th centuries just prior to the Angkor Droughts (1, 3, 11, 12). Channel infill is concurrent with a considerable increase in linear sedimentation and mass accumulation rates in the West Baray, which may suggest enhanced sediment delivery to the barays at that time as well (Fig. 2*A*, Table 2). Overall, sediment delivery to the West Baray was greatest during Angkorian times, particularly in the 13th century, and declined during the post-Angkorian period. Reduced sediment delivery may have been a consequence of drier climate during the LIA or anthropogenic factors, such as cessation of water management, less intense land use, and greater soil stabilization associated with abandonment of the urban area. Higher organic C content in the post-Angkorian portion of the core is consistent with the interpretation of reduced detrital sediment transport to the West Baray.

In addition to diminished sediment delivery, the shift to more radiogenic Sr isotope values in the post-Angkorian period may suggest a change in sediment source (Fig. 2*I*). The $^{87}Sr/^{86}Sr$ increase, however, probably does not reflect a new geographic source of sediments to the baray. Instead, the shift in the Sr isotope ratio in the West Baray core probably indicates delivery of less chemically altered sediments in post-Angkorian times (Fig. S3 and *SI Text*). Reduced weathering could have been the result of less intense land use and greater soil stabilization. Alternatively, wetter conditions during the MCA could have contributed to enhanced weathering during the Angkorian period, followed by less intense weathering during the drier LIA. Overall, the baray sediments suggest a decrease in both erosion and chemical weathering in the watershed postcollapse.

Response to Drought. The West Baray sediment record displays changes in response to three known drought intervals: the early 13th century, the 14th and 15th century Angkor Droughts, and the middle to late 18th century, including the Strange Parallels and East India Droughts (12, 15). During these three periods, both organic C content and C/N ratios increase (Fig. 2 *D* and *E*). West Baray sediments deposited during drought episodes are likely richer in organic matter because of reduced input of detrital sediment and water to the baray. Sediment composition, color, and density are controlled by the relative contribution of authochthonous (limnetic) and allochthonous (detrital) sediments (Fig. S2). Unfortunately, the radiocarbon chronology of the core does not provide the resolution needed to determine whether sedimentation rate decreased during each of the three drought intervals. The linear sedimentation and mass accumulation rates for the relatively organic-rich horizon during and after the Angkor Droughts, however, is much lower than rates during the remainder of the record, suggesting a large reduction in sediment delivery to the baray at that time (Fig. 2*A*). Increased C/N ratios may signal the proliferation of aquatic macrophytes, an expected response to lower water levels and habitat expansion. Floating vegetation was present in the West Mebon basin starting in the 14th century, demonstrating that aquatic macrophytes existed within the baray at that time (17). Although C/N values increase, they do not reach levels indicative of a macrophyte-dominated system (>15). This suggests that at least the deep, southwest corner of the West Baray sustained phytoplankton production throughout the history of the baray. Factor 1 reveals higher abundance of Zr, Ti, Sr, and Rb during at least the first two drought intervals. The scanning XRF data terminate in the 17th century due to poor sediment consolidation and postretrieval disturbance of more recent deposits (Fig. 2 *G* and *H*). Sediments became more coarse grained in the southwest part of the baray during the low stands associated with the period of the Angkor Droughts (Fig. 2 *F* and *G*). This is likely due to decreased input of fines and lowered water levels in the baray that increased turbulence and bottom resuspension. Sediment coarsening is consistent with processes observed in reservoirs during periods of drawdown (20, 21).

Ecological Evolution of the Baray. Higher C/N values after approximately 1300 AD may reflect proliferation of aquatic macrophytes after the collapse of Angkor. Elevated water levels during early, wetter times may have precluded the spread of higher plants into deep-water areas of the baray, where submersed and rooted species would have been light limited, and where depths may have been too great for floating-leaved taxa. The drier climate of the LIA may have lowered water levels in the baray and expanded the habitat available to aquatic macrophytes. Additionally, macrophytes may have been manually removed from the baray during the Angkorian period. Evidence for cessation of vegetation clearance is observed in the West Mebon, where floating vegetation has persisted since the 14th century (17). Biogenic silica

measurements indicate a greater abundance of diatoms from the 16th century onward, whereas sponge spicule abundance decreased (Fig. 3*D*). This finding is confirmed by microscopic analysis of sediments using smear slides (Fig. S4). The increased abundance of diatoms postcollapse is partly attributed to the appearance of several pennate species (Fig. S4). Many pennate diatoms occupy benthic habitats, suggesting an expansion of such habitats postcollapse. Benthic algae tend to thrive when sediment suspension is infrequent, implying relatively lower turbidity in the post-Angkorian West Baray. An inference for more turbid conditions in the West Baray during the Angkorian period is consistent with evidence for relatively high sediment and water delivery to the reservoir at that time. Turbidity may have decreased postcollapse as a consequence of reduced sediment transport to the baray or because the expanded macrophyte community trapped incoming sediments and suppressed sediment resuspension in the southwestern part of the baray. Extensive benthic algae growth may be the cause of higher TP values from the 17th century. Benthic algae can promote oxygenation of the sediment-water interface, which in turn enhances iron-mediated sequestration of P in sediments (22).

The shift to more negative $\delta^{13}C$ and $\delta^{15}N$ values (Fig. 3 *A*, and *B*) postcollapse can be attributed to the change in vegetation within the baray that resulted from lower water levels and cessation of water management. It is also possible the West Baray has become N-limited since the 18th century, as $\delta^{15}N$ values approach 0‰, implying a strong contribution of N-fixing cyanobacteria to sediment organic matter (Fig. 3*B*). Benthic algae growth can inhibit the release of N from the sediments to the water column, which may amplify N limitation in the water column (22). Some aquatic higher plants, however, can have $\delta^{15}N$ values close to 0‰ (23), but the C/N values (<15) of the baray deposits imply that higher plants were not the primary contributor to sediment organic matter.

Comparison to the West Mebon. The West Mebon is a temple located on an artificial island in the center of the West Baray (Fig. 1*C*). Penny et al. (17) recovered a sediment core from a basin enclosed by the temple. Our core has two advantages over the West Mebon record (17) in providing paleoenvironment information about the baray. First, although the West Mebon basin is certainly influenced by the West Baray, it is, as discussed by Penny et al (17), buffered from conditions within the baray and thus would not necessarily record all the fluctuations that may have occurred in the baray itself. Second, the West Mebon core (17) only contains 27.5 cm of material and begins in the 12th century. Our core spans the entire limnetic history of the baray over nearly 190 cm of sediment. These differences in location and resolution are likely the reason for some of the apparent discrepancies between the two records. For example, the West Mebon record (17) indicates a considerable drop in water levels in the baray at the end of the 12th century, likely related to the construction of features such as the Jayatataka baray and the Angkor Thom moat (4) and CP807 (24) (Fig. 1*B*). In contrast, we do not observe any significant variations in conditions in the West Baray until the 13th century when sedimentation rates increase and several parameters respond to a period of drought (Fig. 2 *A*–*G*). Furthermore, in the West Mebon basin, the water depth appears to have risen again in the 14th century. It seems unlikely that water levels in the southwest part of the baray rose during the 14th century given that the increase in % sand fraction during the Angkor Droughts period implies lower water levels (Fig. 2*F*).

Conclusions

This sediment record from the West Baray provides a unique perspective on environmental change at Angkor. Sr isotopes, sedimentation rates, sediment density, composition, and color (reflecting organic matter content), all illustrate that the baray received greater sediment and water input prior to the 14th and 15th century megadroughts and contemporaneous collapse of Angkor. A condensed section with increased sand fraction indicates decreased sediment input and lower water levels in the baray during the Angkor Droughts in the 14th and 15th centuries. Since the 16th century, the baray records a decrease in both physical and chemical weathering within the drainage basin. The ecology of the baray has also changed in post-Angkorian times, as there has been a proliferation of benthic taxa related to reduced water-column turbidity and increased macrophyte growth. Changes in sedimentation and ecology were brought about by complex interactions between natural (climate) and anthropogenic (water management and land use) factors. Our data are unable to distinguish between climatic and anthropogenic forcings, but it is likely these two factors often acted in tandem, as environmental changes would lead to human action regarding the water management network. Nonetheless, the Khmer water management system is a vivid example of a sophisticated human technology that failed in the face of extreme (threshold) environmental conditions.

Methods

Two cores were collected with a piston corer from the southwest corner of the West Baray (13° 25′ 38″ N, 103° 45′ 58″ E) in 6.2 m of water on December 20, 2003. The first, 1.92-m long core WB1-20-XII-03 MWI-1, was obtained using a double 5.7-cm (o.d.) clear polycarbonate tube and transported, intact, to the laboratory. The second, 87-cm long core WB1-20-XII-03 MWI-2, was sampled at 1-cm intervals in the field prior to being transported to the laboratory. All analyses were performed on core WB1-20-XII-03 MWI-1 unless otherwise noted. Sediment density of the first core was measured at 0.5-cm intervals using a GEOTEK Multisensor Core Logger. The core was split lengthwise and imaged using a GEOTEK digital color line-scan camera.

The split core from 0.70 to 1.91 mblf was analyzed with an Avaatech XRF core scanner at 1-cm resolution to provide close-interval elemental data. Measurements of elements Al to Ba were made using a slit size of 1×1 cm and generator settings of 10, 30, and 50 kV over 30 s of counting time. The upper 0.70 m of the archive half of the core were poorly consolidated and disturbed and could not be analyzed (the working half of the core was not affected). Elements were normalized to Al. Normalization to a conservative element such as Al removes inconsistencies in elemental data resulting from changes in sedimentation rates, grain size, and organic matter content (25). The XRF dataset was reduced by factor analysis using Predictive Analytics SoftWare Statistics 18.0. Three factors that explain 82.6% of the variance in the data were extracted using principal components analysis with Varimax rotation.

Sr was separated using cation exchange resin and Sr isotope ratios were measured on a VG Sector 54 TIMS using a triple collector dynamic algorithm, normalized to $^{87}Sr/^{86}Sr$ 0.1194, with an exponential fractionation correction (26). The 90 analyses of National Bureau of Standards reference material 987 during the 2-y period of these analyses gave a mean value of 0.710266 ± 0.000008 (1 sigma). The Sr blanks were negligible in comparison to the Sr content of the samples.

Weight percent C and N of bulk sediment from core WB1-20-XII-03 MWI-2 were measured on a Carlo Erba NA1500 CNS Elemental Analyzer. C/N ratios are expressed as atomic ratios. Stable C and N isotopes were measured on a Costech Elemental Analyser attached to a Thermo Delta V mass spectrometer. Analytical precision for $\delta^{13}C$ was better than ±0.10‰, and for $\delta^{15}N$ better than ±0.15‰. Samples analyzed for total P were digested in 5.0% H_2SO_4 and 5.0% K_2SO_8 in an autoclave and measured using a Bran–Luebbe Autoanalyzer (27). Biogenic Si (diatoms and sponge) was determined using time-course leaching (28). Weight percent coarse fraction (>63 μm) was determined by wet sieving and weighing the dried >63 μm fraction.

Radiocarbon dates were obtained on chemically pretreated wood and decarbonated bulk sediment samples at the Center for Accelerator Mass Spectrometry (CAMS) at Lawrence Livermore National Laboratories and the Natural Environment Research Council (NERC) Radiocarbon Facility (Environment) and Scottish Universities Environmental Research Centre (SUERC) Accelerator Mass Spectrometry Laboratory. Bulk sediment samples processed at CAMS were decarbonated using 1 N·HCl with vortexing to prevent clumping, spun down, decanted, and rinsed three times with Milli-Q water. The sediment was then dried overnight on a heating block and converted to carbon dioxide (CO_2) in individual quartz tubes using copper oxide (CuO) as an oxygen source. Wood samples received a modified "deVries" chemical

pretreatment and an acid–base–acid treatment at 90 °C, followed by copious rinsing with Milli-Q water. Bulk sediment samples processed at the NERC Radiocarbon Facility (Environment) were digested in 2 M HCl at 80 °C for 8 h, then washed with deionized water and dried and homogenized. Samples were converted to CO_2 by heating with CuO in sealed quartz tubes and the gas was converted to graphite by Fe/Zn reduction. Dates were calibrated to calendar years before present using Calib html version 6.0 (29) that uses the IntCal09 radiocarbon calibration curve (30).

ACKNOWLEDGMENTS. We thank Thomas P. Guilderson for his generous assistance with radiocarbon dates. Sarah Metcalfe kindly provided help with diatom identification. Two anonymous reviewers provided constructive comments that greatly improved the clarity of this paper. We are also indebted to Christophe Pottier and Dominique Soutif for discussions that strengthened the manuscript. We thank the Authority for the Protection and Management of Angkor and the Region of Siem Reap for permission to work in the Angkor Archaeological Park, and we appreciate support from l'École Française d'Extrême-Orient. We are grateful for funding from the Gates Cambridge Trust (M.B.D.), Natural Environment Research Council Radiocarbon Award 1452.1009 (D.A.H.), and the Adolph and Marion Lichstern Fund of the Department of Anthropology, University of Chicago that supported fieldwork and additional radiocarbon dates (A.L.K.).

1. Evans D, et al. (2007) A comprehensive archaeological map of the world's largest preindustrial settlement complex at Angkor, Cambodia. *Proc Natl Acad Sci USA* 104:14277–14282.
2. Fletcher RJ, et al. (2003) Redefining Angkor: structure and environment in the largest, low density urban complex of the pre-industrial world. *Udaya* 4:107–121.
3. Fletcher R, et al. (2008) The water management network of Angkor, Cambodia. *Antiquity* 82:658–670.
4. Fletcher R, Pottier C, Evans D, Kummu M (2008) The development of the water management system of Angkor: A provisional model. *IPPA Bull* 28:57–66.
5. Kummu M (2009) Water management in Angkor: Human impacts on hydrology and sediment transport. *J Environ Manage* 90:1413–1421.
6. Acker R (1998) New geographical tests of the hydraulic thesis at Angkor. *South East Asia Research* 6:5–47.
7. van Liere WJ (1980) Traditional water management in the lower Mekong Basin. *World Archaeol* 11:265–280.
8. Groslier BP (1979) La cité hydraulique angkorienne: exploitation ou surexploitation du sol? *Bulletin de l'École française d'Extrême-Orient* 66:161–202.
9. Pottier C (1999) Carte archéologique de la région d'Angkor Zone sud. PhD thesis (Universite Paris III Sorbonne Nouvelle, Paris).
10. Pottier C (2000) Some evidence of an Inter-relationship between hydraulic features and rice field patterns at Angkor during ancient times. *The Journal of Sophia Asian Studies* 18:99–119.
11. Coe MD (2003) *Angkor and the Khmer Civilization* (Thames and Hudson, London).
12. Buckley BM, et al. (2010) Climate as a contributing factor in the demise of Angkor, Cambodia. *Proc Natl Acad Sci USA* 107:6748–6752.
13. Lustig T, Fletcher R, Kummu M, Pottier C, Penny D (2008) *Modern Myths of the Mekong: A critical review of water and development concepts, principles and policies*, eds M Kummu, M Keskinen, and O Varis (Helsinki University of Technology Water and Development Publications, Espoo, Finland), pp 81–94.
14. Yan H, et al. (2011) South China Sea hydrological changes and Pacific Walker Circulation variations over the last millennium. *Nat Commun* 2:293.
15. Cook ER, et al. (2010) Asian monsoon failure and megadrought during the last millennium. *Science* 328:486–489.
16. Someth P, Kubo N, Tanji H (2007) A combined technique of floodplain storage and irrigation for paddy rice cultivation. *Paddy Water Environ* 5:101–112.
17. Penny D, et al. (2007) Hydrological history of the West Baray, Angkor, revealed through palynological analysis of sediments from the West Mebon. *Bulletin de l'École Française d'Extrême-Orient* 92:497–521.
18. Tsukawaki S, Okuno M, Okawara M, Kato M, Nakamura T (1998) Underground structures of the site of East Baray Reservoir in the Angkor district, central Cambodia. *Summaries of researchers using AMS at Nagoya University* 9:272–280.
19. Pottier C, et al. (2004) Koh Ta Méas, un site préhistorique dans le baray occidental rapport préliminaire. *Udaya* 5:167–191.
20. Morris GL, Fan J (1998) *Reservoir Sedimentation Handbook* (McGraw-Hill Book Co, New York).
21. Shotbolt LA, Thomas AD, Hutchinson SM (2005) The use of reservoir sediments as environmental archives of catchment inputs and atmospheric pollution. *Prog Phys Geog* 29:337–361.
22. Scheffer M (1998) *Ecology of Shallow Lakes* (Kluwer Academic Publishers, London).
23. Brenner M, et al. (2006) Mechanisms for organic matter and phosphorus burial in sediments of a shallow, subtropical, macrophyte-dominated lake. *J Paleolimnol* 35:129–148.
24. Pottier C (2006) Searching for Goloupura. *Proceedings of the Phnom Bakheng Workshop on Public Interpretation* (Center for Khmer Studies, Siem Reap, Cambodia), pp 41–72.
25. Löwemark L, et al. (2011) Normalizing XRF-scanner data: A cautionary note on the interpretation of high-resolution records from organic-rich lakes. *J Asian Earth Sci* 40:1250–1256.
26. Bickle MJ, et al. (2003) Fluxes of Sr into the headwaters of the Ganges. *Geochim Cosmochim Acta* 67:2567–2584.
27. Kenney WF, Schelske CL, Chapman AD (2001) Changes in polyphosphate sedimentation: a response to excessive phosphorus enrichment in a hypereutrophic lake. *Can J Fish Aquat Sci* 58:879–887.
28. Conley DJ, Schelske CL (1993) Potential role of sponge spicules in influencing the silicon biogeochemistry of Florida lakes. *Can J Fish Aquat Sci* 50:296–302.
29. Stuiver M, Reimer PJ (1993) Extended ^{14}C database and revised CALIB radiocarbon calibration program. *Radiocarbon* 35:215–230.
30. Reimer PJ, et al. (2009) IntCal09 and Marine09 radiocarbon age calibration curves, 0–50,000 years cal BP. *Radiocarbon* 51:1111–1150.